

Evidence of a critical hole concentration in underdoped $\text{YBa}_2\text{Cu}_3\text{O}_y$ single crystals revealed by ^{63}Cu NMR

S.-H. Baek,^{1,*} T. Loew,² V. Hinkov,^{2,3} C. T. Lin,² B. Keimer,² B. Büchner,^{1,4} and H.-J. Grafe¹

¹*IFW-Dresden, Institute for Solid State Research, PF 270116, 01171 Dresden, Germany*

²*Max-Planck-Institut für Festkörperforschung, Heisenberg-strasse 1, 70569 Stuttgart, Germany*

³*Quantum Matter Institute, University of British Columbia, 2355 East Mall, Vancouver, Canada V6T 0A5*

⁴*Institut für Festkörperphysik, Technische Universität Dresden, 01062 Dresden, Germany*

(Received 7 March 2012; revised manuscript received 28 November 2012; published 13 December 2012)

We report a ^{63}Cu NMR investigation in detwinned $\text{YBa}_2\text{Cu}_3\text{O}_y$ single crystals, focusing on the highly underdoped regime ($y = 6.35\text{--}6.6$). Measurements of both the spectra and the spin-lattice relaxation rates of ^{63}Cu uncover the emergence of static order at a well-defined onset temperature T_0 with an as yet unknown order parameter. While T_0 is rapidly suppressed with increasing hole doping concentration p , the spin pseudogap was identified only near and above the doping content at which $T_0 \rightarrow 0$. Our data indicate the presence of a critical hole doping $p_c \sim 0.1$, which may control both the static order at $p < p_c$ and the spin pseudogap at $p > p_c$.

DOI: [10.1103/PhysRevB.86.220504](https://doi.org/10.1103/PhysRevB.86.220504)

PACS number(s): 74.72.Gh, 74.25.N-, 74.40.Kb, 76.60.-k

The superconducting copper oxides (cuprates) in the underdoped regime feature unusual states of matter, such as a pseudogap (PG), density-wave order (stripes), and the coexistence of magnetism and superconductivity. Debates regarding the origin and the precise nature of those phases or related phenomena such as a reconstruction of the Fermi surface at a quantum critical point are still ongoing.¹⁻³ In particular, interest in the underdoped $\text{YBa}_2\text{Cu}_3\text{O}_y$ (YBCO_y) has been revived in recent years, during which significant progress in understanding those subjects has been made through experimental observations of an electric liquid crystal (ELC) or nematic phase,^{4,5} quantum oscillations above a critical doping,⁶⁻⁸ and field-induced charge stripe order.^{9,10}

Motivated by the recent literature and by the available high-quality single crystals of underdoped YBCO_y, we carried out a ^{63}Cu NMR study of YBCO_y to elucidate the underlying physics in the highly underdoped region of the compound on a microscopic level. While nuclear magnetic resonance (NMR) is a powerful local probe, so far, the majority of the NMR studies on the planar Cu in YBCO_y has been performed on nearly optimal or slightly underdoped regions,^{11,12} largely due to strong magnetism which causes complicated static and dynamic effects on NMR parameters. In this Rapid Communication, we show that a critical hole doping p_c exists in the p - T phase diagram of YBCO_y beneath the superconducting (SC) dome at $p \sim 0.1$, below which a static order sets in and above which a spin pseudogap (PG) opens up in the low-energy spin excitation spectrum.

The growth and characterization of detwinned YBCO_y single crystals are described in Refs. 13 and 14. The single crystals investigated here have $y = 6.35$ ($T_c = 10$ K, $p = 0.062$), 6.4 ($T_c = 21$ K, $p = 0.075$), 6.45 ($T_c = 35$ K, $p = 0.082$), 6.5 [sample 1 with short ortho-II correlation length: $T_c = 53$ K, $p = 0.106$; sample 2 with long correlation length (~ 100 Å): $T_c = 61$ K, $p = 0.114$], and 6.6 ($T_c = 61$ K, $p = 0.135$), where p is the hole concentration per planar Cu determined from the c -axis lattice constant.¹⁶ ^{63}Cu NMR spectra were obtained by integrating averaged spin-echo signals as the frequency was swept, and the spin-lattice relaxation rates T_1^{-1}

were measured by monitoring the recovery of the nuclear magnetization after a saturation pulse.

Figure 1 shows ^{63}Cu spectra for $y = 6.35$ and 6.45 measured at $H = 7$ T applied along the c axis. The leftmost sharp line and the rightmost broad line in each panel are identified to arise from the $\text{Cu}(1)_0$ and $\text{Cu}(1)_2$ sites, respectively, in the CuO chains, where the subscript denotes the number of the nearest neighboring oxygen ions *along* the chain.¹⁷ While the central line at room temperature comes from the planar $\text{Cu}(2)$ site,¹⁷ we find that it evolves in a complicated way as T is lowered, especially for $y = 6.35$ and $y = 6.4$.¹⁴ The intensity of $\text{Cu}(2)$ (dotted line in Fig. 1) is strongly suppressed, and at the same time a feature sp_0 , consisting of two resonance lines indicated by two dashed lines, emerges at an onset temperature.¹⁴ Clearly, for $y = 6.45$, sp_0 occurs at a much lower temperature than for $y = 6.35$. The rapid suppression of $\text{Cu}(2)$ with decreasing T is attributed to the *wipeout effect*, as observed in ^{63}Cu NQR in $\text{Y}_{1-z}\text{Ca}_z\text{Ba}_2\text{Cu}_3\text{O}_y$,¹⁸ which arises from a slowing down of spin fluctuations.^{19,20} In contrast, the T dependence of the ^{63}Cu spectra for both $y = 6.5$ and 6.6 are almost identical without any signature of either sp_0 or wipeout of $\text{Cu}(2)$, except for a moderate broadening with decreasing T .¹⁴ Interestingly, we observed the splitting of the $\text{Cu}(1)_2$ line at low T for $y = 6.35$, which may suggest that sp_0 influences $\text{Cu}(1)_2$. In addition, it is noticeable that both sp_0 and $\text{Cu}(1)_0$ broaden significantly at low T below 20 K for $y = 6.35$, suggesting the occurrence of glassy or incommensurate magnetic order. Note that such a broadening could not be measured for $y = 6.4$ and 6.45, because the magnetic order occurs deep in the superconducting state where the NMR spectra significantly weaken and become complicated.

Figure 2 shows the recovery of the ^{63}Cu nuclear magnetization after a saturating pulse as a function of delay time t at various temperatures for $y = 6.35$ and 6.45, measured at the $\text{Cu}(2)$ line. Unexpectedly, we found a steplike feature in the data, which indicates two T_1 processes. The long T_1 process becomes discernible at 265 K for $y = 6.35$ and at 120 K for 6.45, and its fraction [i.e., $1 - m(t)$ at the step] increases rapidly with decreasing T . Comparing with the T dependence of the spectrum as shown in Fig. 1, we find that

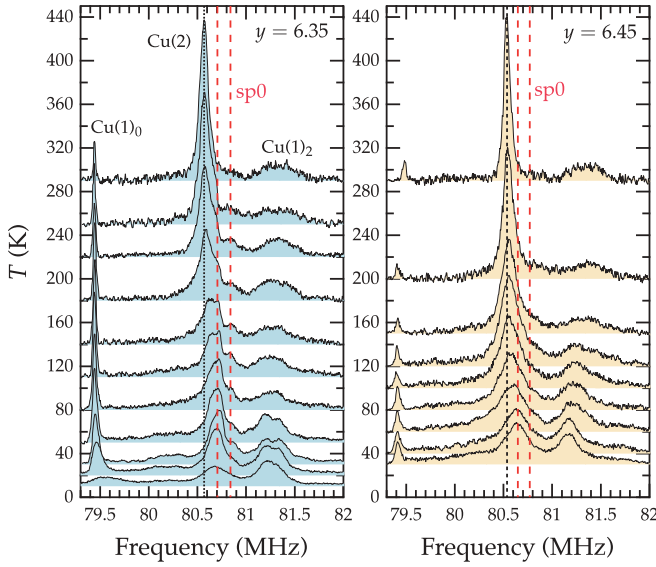


FIG. 1. (Color online) ^{63}Cu NMR spectra in YBCO_y at 7 T along the c axis for $y = 6.35$ (left panel) and $y = 6.45$ (right panel). Cu(1) denotes the Cu sites in the CuO chains, where the subscripts 0 and 2 represent the number of neighboring oxygen ions along the chain, and Cu(2) (dotted lines) denotes the planar Cu sites (Ref. 17). An emerging Cu spectral feature sp0 consisting of two resonance lines indicated by two dashed lines is clearly visible for $y = 6.35$. The horizontal bar indicates the region that was irradiated during a T_1 measurement. See Supplemental Material for details and for other doping levels (Ref. 14).

the long $T_{1\ell}$ component arises when the spectrum sp0 becomes visible, suggesting that sp0 is due to an emerging static phase featured by the long $T_{1\ell}$.¹⁴ Since two T_1 processes are evident in the relaxation data, we used a fitting function for magnetic relaxation of the central transition for $I = 3/2$ including two T_1 components,

$$m(t) = [1 - a\{(1 - w)(0.1e^{-t/T_{1s}} + 0.9e^{-6t/T_{1s}}) + w(0.1e^{-t/T_{1\ell}} + 0.9e^{-6t/T_{1\ell}})\}], \quad (1)$$

where a is a fitting parameter which is ideally one for saturation recovery. T_{1s} ($T_{1\ell}$) are the short (long) T_1 components, and w is the fraction of the volume governed by the long $T_{1\ell}$ process to the total volume. The solid curves in Fig. 2 are fits to Eq. (1). At low T (≤ 70 K), it was necessary to impose the stretching exponent β in Eq. (1) for the $T_{1\ell}$ recovery, which is indicative of a crossover to a glassy magnetic phase.

The resulting $(T_{1s}T)^{-1}$, $(T_{1\ell}T)^{-1}$, and w as a function of T and for all y are presented in Fig. 3. The results in $\text{YBCO}_{6.6}$ are compatible with data known so far,¹⁷ revealing the spin pseudogap with the onset $T^* \sim 145$ K. The spin-lattice relaxation rate probes the gap solely in the spin excitation spectrum since $(T_1T)^{-1} \propto \sum_{\mathbf{q}} A^2(\mathbf{q})\chi''(\mathbf{q}, \omega_0)$, where $A(\mathbf{q})$ is the hyperfine coupling constant and ω_0 the Larmor frequency. Therefore, the onset temperature of the PG and its doping dependence obtained by $(T_1T)^{-1}$ can be significantly different from those obtained by the Knight shift, which probes the spin response at $\mathbf{q} = 0$ only,¹⁸ and other techniques such as angle-resolved photoemission spectroscopy (ARPES) and optical conductivity which probe the charge gap.¹ For $\text{YBCO}_{6.5}$, T^* is reduced to ~ 110 K, as indicated by arrows. We performed

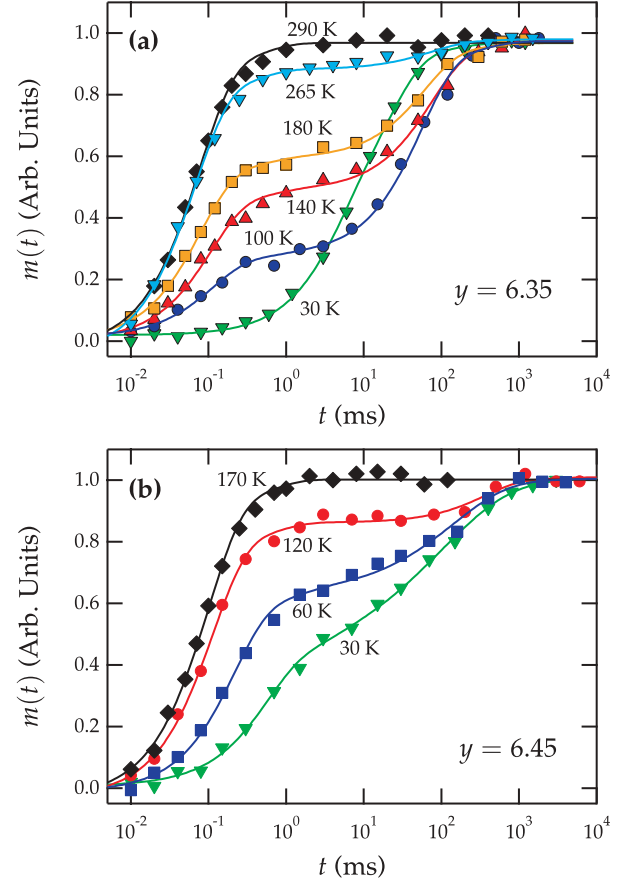


FIG. 2. (Color online) Recovery of the (normalized) nuclear magnetization $m(t)$ as a function of time t for $y = 6.35$ (a) and $y = 6.45$ (b). In (a), $m(t)$ deviates progressively from a single T_1 process with decreasing T , revealing the long $T_{1\ell}$ process which overwhelms the short one at low T . Note that the short T_{1s} component is no longer detectable at 30 K. In (b), the $T_{1\ell}$ process is strongly suppressed, i.e., it appears below ~ 150 K and a large portion of the T_{1s} process remains down to 30 K. The solid lines are fits to Eq. (1).

the measurement in another $\text{YBCO}_{6.5}$ crystal which has a longer ortho-II correlation length ~ 100 Å. For this sample, both p and T_c turn out to be larger than the sample with a shorter correlation length, being consistent with slightly larger T^* . Upon further lowering y to 6.45, $(T_{1\ell}T)^{-1}$ increases with decreasing T , reaching a plateau below ~ 150 K, which is in contrast to the pseudogap behavior reported in a similarly doped compound.²¹ $(T_{1s}T)^{-1}$ of $\text{YBCO}_{6.35}$ and $\text{YBCO}_{6.4}$ is further enhanced with no signature of the PG as well, although T_{1s} is not measurable below 100 and 50 K, respectively, due to limited experimental resolution [see Fig. 2(a)]. Note that the T dependence of the data undergoes a dramatic change as y is reduced from 6.5 to 6.45, implying the existence of a critical doping just below $y = 6.5$.

Figure 3(b) shows the long relaxation rate $(T_{1\ell}T)^{-1}$ vs T which arises from the sp0 line. For comparison, the corresponding $(T_{1s}T)^{-1}$ data of Cu(2) are also shown. ($T_{1\ell}$ is not detected for $y = 6.5$ and 6.6.) In $\text{YBCO}_{6.35}$, $(T_{1\ell}T)^{-1}$ is almost constant at high T , but it starts to rise steeply below ~ 100 K, forming a sharp peak centered at ~ 11 K. These behaviors, together with the significant broadening

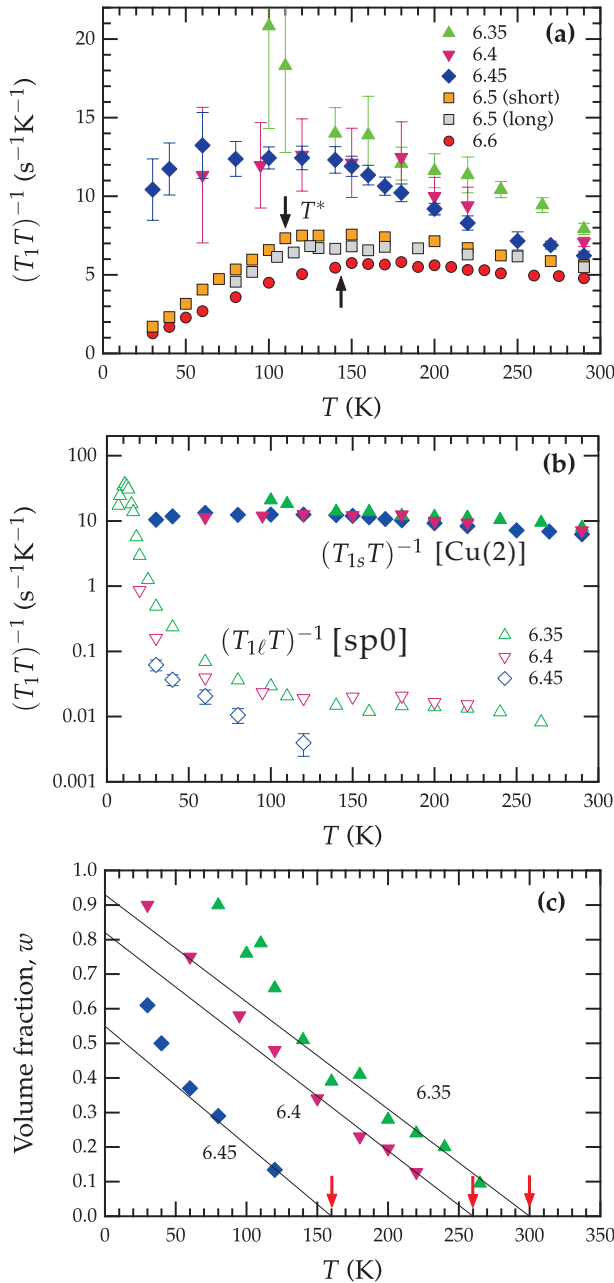


FIG. 3. (Color online) (a) Nuclear spin-lattice relaxation rates divided by T , $(T_1T)^{-1}$ vs T for the short T_{1s} . The opening of the PG at T^* (denoted by arrows) was detected only for $y \geq 6.5$, whereas there are no signatures of the PG for $y \leq 6.45$. In (b), $(T_{1\ell}T)^{-1}$ data are presented, together with $(T_{1s}T)^{-1}$, for comparison. In $\text{YBCO}_{6.35}$, $(T_{1\ell}T)^{-1}$ forms a local maximum at $T_g \sim 11$ K, indicating a SG transition. This behavior is significantly suppressed for $y = 6.45$. (c) T dependence of the volume fraction w . The onset temperature T_0 is defined from the values at which $w \rightarrow 0$ (down arrows).

of the spectra at low T , lead to the conclusion that a spin freezing or spin-glass (SG) transition occurs at a characteristic temperature $T_g \sim 11$ K for $y = 6.35$. We find that our data resembles the results of ^{89}Y NMR in $\text{Y}_{1-z}\text{Ca}_z\text{Ba}_2\text{Cu}_3\text{O}_y$ (Ref. 18) and ^{139}La NQR/NMR in $\text{La}_{2-x}\text{Sr}_x\text{CuO}_4$.^{22,23} Similar T dependencies of $(T_{1\ell}T)^{-1}$ were also observed for $y = 6.4$ and 6.45 . Although we were not able to identify the local

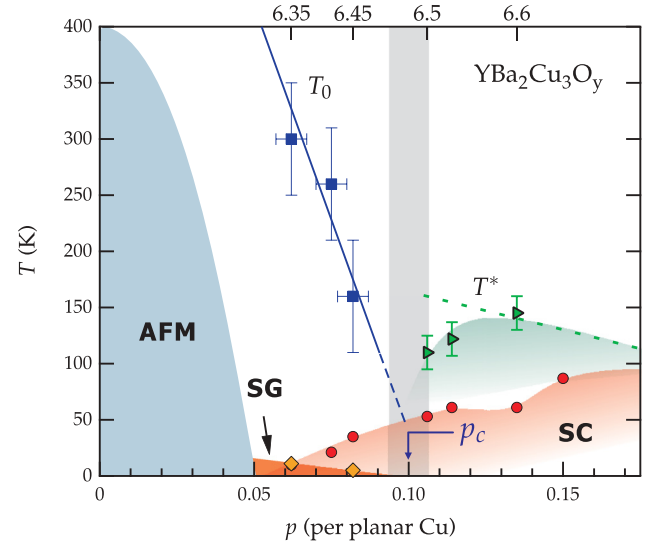


FIG. 4. (Color online) Phase diagram of underdoped YBCO_y in terms of hole concentration p . y values are shown on the top axis for convenience. The antiferromagnetic (AFM) transition is from Ref. 13 and the dotted line drawn for T^* is estimated from previously known NMR results (Refs. 11 and 18).

maximum for these doping levels due to the higher T_c which complicates the identification of T_g by NMR, one can obtain $T_g \sim 5$ K for $y = 6.45$ from the muon spin rotation (μSR) study of $\text{Y}_{1-x}\text{Ca}_x\text{Ba}_2\text{Cu}_3\text{O}_6$, which shows a very similar p dependence of T_g .²⁴

Figure 3(c) shows the volume fraction w as a function of T , obtained from the fit of relaxation data $m(t)$ using Eq. (1). It should be emphasized that the values of w themselves have no quantitative meaning, since they may depend on the frequency at which the relaxation rates were measured. Moreover, the wipeout of Cu(2) should lead to a significant increase of w , particularly at low T , which is indeed thought to account for the rapid increase of w at low temperatures [see Fig. 3(c)]. Nonetheless, the temperature at which $w \rightarrow 0$, i.e., where the $T_{1\ell}$ process vanishes with increasing T , should be unaffected by those facts. Thus, with reasonable accuracy, one can define the onset temperature T_0 from the values extrapolated to $w = 0$, denoted by arrows.

From these results, we draw the p - T phase diagram in Fig. 4. The most striking feature is that T_0 falls rapidly to zero at a hole concentration of $p \sim 0.1$ beneath the SC dome. At the same time, the SG transition temperature T_g shows also a similar doping dependence, being terminated at p where $T_0 \rightarrow 0$. These behaviors suggest a close relationship between T_0 and T_g , collapsing to the same critical doping $p_c \sim 0.1$. Interestingly, it turns out that p_c is very near the doping level at which the metal-insulator crossover (MIC) takes place²⁵ or the Fermi surface is reconstructed by density-wave order.^{8,9,26} The phase diagram is also in qualitative agreement with that suggested by inelastic neutron scattering (INS) and μSR studies.^{13,27}

A remarkable finding in our study is that the *spin* pseudogap is observed only near and above p_c (i.e., $y \geq 6.5$) [see Figs. 3(a) and 4]. Note that T^* of $\text{YBCO}_{6.5}$ positioned near p_c is much lower than the value expected based on extrapolation

of the doping dependence established at higher p , which is indicated by the dotted line. Indeed, the sudden drop of T^* near p_c in YBCO_{6.5} appears as a crossover to the absence of T^* in YBCO_{6.45}, corroborating the INS results in which the suppression of the low-energy spin excitations (i.e., spin pseudogap) was not detected down to 5 K in YBCO_{6.45}.^{5,28,29} Such an abrupt suppression of the spin pseudogap *below a critical doping level* was reported in NMR studies not only of similarly hole-doped $Y_{1-z}Ca_zBa_2Cu_3O_y$ (Ref. 18) but also of the multilayer cuprate $Ba_2Ca_2Cu_3O_6(F_yO_{1-y})_2$.³⁰ By the same token, the fact that p_c is in the vicinity of the MIC²⁵ agrees well with the disappearance of the quantum oscillations below $\sim p_c$, as well as with the NMR result in $Bi_2Sr_{2-x}La_xCuO_{6+\delta}$ that the ground state of the PG is metallic.³¹ Therefore, we argue that the spin PG phenomenon may be quantum critical, stemming from the suppression of magnetism. In fact, such a strong competition between magnetism and the PG gives a good account of the observation that the PG is abruptly suppressed by substituting the Cu(2) sites with $\sim 1\%$ Zn impurities around which a local moment is induced on the Cu(2) sites in YBCO_{6.7} (Ref. 32) and $YBa_2Cu_4O_8$.³³

While the nature of static order which appears at T_0 is yet unclear, one may consider T_0 as the onset of stripelike charge modulation in the plane, possibly induced by the end Cu ion of the oxygen-filled chains, Cu(1)₁. In fact, as effective impurities, Cu(1)₁ sites can cause Friedel-like oscillations,³⁴ which may in turn induce the stripelike charge modulation in the plane. This would be consistent with a higher T_0 at lower p , where the number of Cu(1)₁ is higher. The charge modulation

scenario agrees well with signatures of broken rotational symmetry observed in resistivity⁴ and INS^{5,13} measurements at $p < p_c$. In this case, the planar Cu(2) sites should be differentiated into two spatially modulated distinct regions. In terms of stripes, the short T_{1s} -yielding region is naturally related to spin stripes which consist of the localized Cu(2) spins, while charge stripes may yield the long $T_{1\ell}$ if the spin contributions to the relaxation rates were almost quenched. Although the stripelike charge modulation accounts for our results to a large extent, it remains a question as to whether the two alternating regions in the stripe structure could, in practice, result in the $(T_{1s}T)^{-1}$ and $(T_{1\ell}T)^{-1}$ values that strikingly differ up to three orders of magnitude.

In summary, we performed a systematic ⁶³Cu NMR study as a function of doping and temperature in highly underdoped $YBa_2Cu_3O_y$, showing that static order, probably stripelike, emerges at the onset temperature T_0 , being followed by glassy magnetic order at T_g . The resulting phase diagram includes a critical hole doping $p_c \sim 0.1$, at which both T_0 and T_g fall to zero. Another important finding is that the spin pseudogap was detected only above p_c , suggesting that the spin pseudogap phase competes with the magnetic order and/or the static order detected at T_g and T_0 , respectively.

We thank M. Vojta, M.-H. Julien, and N. J. Curro for useful suggestions and discussion, and D. Paar for experimental help. This work has been supported by the Deutsche Forschungsgemeinschaft (DFG) through FOR 538 (Grant No. BU887/4) and SPP1458 (Grant No. GR3330/2).

*sbaek.fu@gmail.com

¹M. R. Norman, D. Pines, and C. Kallin, *Adv. Phys.* **54**, 715 (2005).

²M. Vojta, *Adv. Phys.* **58**, 699 (2009).

³L. Taillefer, *J. Phys.: Condens. Matter* **21**, 164212 (2009).

⁴Y. Ando, K. Segawa, S. Komiya, and A. N. Lavrov, *Phys. Rev. Lett.* **88**, 137005 (2002).

⁵V. Hinkov, D. Haug, B. Fauque, P. Bourges, Y. Sidis, A. Ivanov, C. Bernhard, C. T. Lin, and B. Keimer, *Science* **319**, 597 (2008).

⁶N. Doiron-Leyraud, C. Proust, D. LeBoeuf, J. Levallois, J.-B. Bonnemaison, R. Liang, D. A. Bonn, W. N. Hardy, and L. Taillefer, *Nature (London)* **447**, 565 (2007).

⁷S. E. Sebastian, N. Harrison, M. M. Altarawneh, C. H. Mielke, R. Liang, D. A. Bonn, and G. G. Lonzarich, *Proc. Natl. Acad. Sci. USA* **107**, 6175 (2010).

⁸D. LeBoeuf, N. Doiron-Leyraud, B. Vignolle, M. Sutherland, B. J. Ramshaw, J. Levallois, R. Daou, F. Laliberté, O. Cyr-Choinière, J. Chang *et al.*, *Phys. Rev. B* **83**, 054506 (2011).

⁹F. Laliberté, J. Chang, N. Doiron-Leyraud, E. Hassinger, R. Daou, M. Rondeau, B. Ramshaw, R. Liang, D. Bonn, W. Hardy *et al.*, *Nat. Commun.* **2**, 432 (2011).

¹⁰T. Wu, H. Mayaffre, S. Kramer, M. Horvatic, C. Berthier, W. N. Hardy, R. Liang, D. A. Bonn, and M.-H. Julien, *Nature (London)* **477**, 191 (2011).

¹¹A. Rigamonti, F. Borsa, and P. Carretta, *Rep. Prog. Phys.* **61**, 1367 (1998).

¹²R. E. Walstedt, *The NMR Probe of High- T_c Materials* (Springer, Berlin, 2008).

¹³D. Haug, V. Hinkov, Y. Sidis, P. Bourges, N. B. Christensen, A. Ivanov, T. Keller, C. T. Lin, and B. Keimer, *New J. Phys.* **12**, 105006 (2010).

¹⁴See Supplemental Material at <http://link.aps.org/supplemental/10.1103/PhysRevB.86.220504> for details of sample characterization and additional ⁶³Cu NMR spectra as a function of doping, temperature, repetition time, and external field.

¹⁵For intermediate oxygen concentrations, superstructures can be formed in the CuO chains. For $x = 6.5$, every second chain is empty (ortho-II phase), and the correlation length specifies the range of ordering.

¹⁶R. Liang, D. A. Bonn, and W. N. Hardy, *Phys. Rev. B* **73**, 180505 (2006).

¹⁷M. Takigawa, A. P. Reyes, P. C. Hammel, J. D. Thompson, R. H. Heffner, Z. Fisk, and K. C. Ott, *Phys. Rev. B* **43**, 247 (1991).

¹⁸P. M. Singer and T. Imai, *Phys. Rev. Lett.* **88**, 187601 (2002).

¹⁹A. W. Hunt, P. M. Singer, K. R. Thurber, and T. Imai, *Phys. Rev. Lett.* **82**, 4300 (1999).

²⁰N. J. Curro, P. C. Hammel, B. J. Suh, M. Hücker, B. Büchner, U. Ammerahl, and A. Revcolevschi, *Phys. Rev. Lett.* **85**, 642 (2000).

²¹C. Berthier, M. H. Julien, O. Bakharev, M. Horvatic, and P. Ségransan, *Physica C* **282–287**, 227 (1997).

²²F. C. Chou, F. Borsa, J. H. Cho, D. C. Johnston, A. Lascialfari, D. R. Torgeson, and J. Ziolo, *Phys. Rev. Lett.* **71**, 2323 (1993).

- ²³M.-H. Julien, F. Borsa, P. Carretta, M. Horvatić, C. Berthier, and C. T. Lin, *Phys. Rev. Lett.* **83**, 604 (1999).
- ²⁴C. Niedermayer, C. Bernhard, T. Blasius, A. Golnik, A. Moodenbaugh, and J. I. Budnick, *Phys. Rev. Lett.* **80**, 3843 (1998).
- ²⁵X. F. Sun, K. Segawa, and Y. Ando, *Phys. Rev. Lett.* **93**, 107001 (2004).
- ²⁶G. Ghiringhelli, M. Le Tacon, M. Minola, S. Blanco-Canosa, C. Mazzoli, N. B. Brookes, G. M. De Luca, A. Frano, D. G. Hawthorn, F. He *et al.*, *Science* **337**, 821 (2012).
- ²⁷F. Coneri, S. Sanna, K. Zheng, J. Lord, and R. De Renzi, *Phys. Rev. B* **81**, 104507 (2010).
- ²⁸J. Rossat-Mignod, L. P. Regnault, C. Vettier, P. Bourges, P. Burllet, J. Bossy, J. Y. Henry, and G. Lapertot, *Physica C* **185–189**, 86 (1991).
- ²⁹S. Li, Z. Yamani, H. J. Kang, K. Segawa, Y. Ando, X. Yao, H. A. Mook, and P. Dai, *Phys. Rev. B* **77**, 014523 (2008).
- ³⁰S. Shimizu, S.-i. Tabata, H. Mukuda, Y. Kitaoka, P. M. Shirage, H. Kito, and A. Iyo, *Phys. Rev. B* **83**, 214514 (2011).
- ³¹S. Kawasaki, C. Lin, P. L. Kuhns, A. P. Reyes, and G.-q. Zheng, *Phys. Rev. Lett.* **105**, 137002 (2010).
- ³²M.-H. Julien, T. Fehér, M. Horvatić, C. Berthier, O. N. Bakharev, P. Ségransan, G. Collin, and J.-F. Marucco, *Phys. Rev. Lett.* **84**, 3422 (2000).
- ³³G. qing Zheng, T. Odaguchi, T. Mito, Y. Kitaoka, K. Asayama, and Y. Kodama, *J. Phys. Soc. Jpn.* **62**, 2591 (1993).
- ³⁴Z. Yamani, B. W. Statt, W. A. MacFarlane, R. Liang, D. A. Bonn, and W. N. Hardy, *Phys. Rev. B* **73**, 212506 (2006).